scientific reports

Check for updates

OPEN

Decreasing matrix effects for accurate analysis of primary aliphatic amines in skin moisturizers using magnetic adsorbent

Mir Ali Farajzadeh[1,2]✉, Sina Mohammad Mehri[1] & Mohammad Reza Afshar Mogaddam[3,4,5]

In this study, for analysis of primary aliphatic amines present in skin moisturizer samples, a dispersive micro solid phase extraction method using a mercaptoacetic acid-modified magnetic adsorbent (MAA@Fe_3O_4) was developed to eliminate matrix effects (while not adsorbing the studied analytes). This approach was combined with vortex-assisted liquid-liquid microextraction for the simultaneous derivatization and extraction of primary aliphatic amines present in these samples. To confirm the successful synthesis of the adsorbent, various characterization techniques were employed, including X-ray diffraction, Brunauer-Emmett-Teller surface area analysis, scanning electron microscopy, Fourier transform infrared spectrometry, energy-dispersive X-ray, thermogravimetric analysis, and vibrating sample magnetometry. ComplexGAPI software and analytical eco-scale index were employed to evaluate the greenness of the method. All key parameters affecting matrix cleanup, derivatization, and extraction were optimized. A gas chromatograph equipped with a flame ionization detector was used for the identification and quantification of the amine derivatives. The method demonstrated high unadsorbed percentage of the analytes (92–97%), significant enrichment factors (420–525), wide linear ranges (1.6–10,000 µg L^{-1}), excellent precision (1.4–2.7%), and low limits of detection (0.5–0.82 µg L^{-1}). This approach offered several advantages, including eco-friendliness, short extraction time, high matrix removal efficiency, simplicity, excellent precision, no need for specialized equipment, and adsorbent reusability for up to five cycles. The method also proved highly effective in the simultaneous extraction and derivatization of amines, further highlighting its potential for analytical applications.

Keywords Primary aliphatic amine, Dispersive micro solid phase extraction, Skin moisturizer, Magnetic adsorbent, Vortex-assisted liquid-liquid Microextraction, Gas chromatography

Abbreviations

PAA	Primary aliphatic amine
DµSPE	Dispersive micro solid phase extraction
VALLME	Vortex-assisted liquid-liquid microextraction
GC	Gas chromatography
FID	Flame ionization detector
EF	Enrichment factor
ER	Extraction recovery
RSD	Relative standard deviation
LR	Linear range
LOD	Limit of detection
LOQ	Limit of quantification

[1]Department of Analytical Chemistry, Faculty of Chemistry, University of Tabriz, Tabriz, Iran. [2]Engineering Faculty, Near East University, Mersin 10, Nicosia 99138, North Cyprus, Turkey. [3]Food and Drug Safety Research Center, Tabriz University of Medical Sciences, Tabriz, Iran. [4]Chemistry and Chemical Engineering Department, Khazar University, 41 Mehseti Street, Baku AZ1096, Azerbaijan. [5]Pharmaceutical Analysis Research Center, Tabriz University of Medical Sciences, Tabriz, Iran. ✉email: mafarajzadeh@yahoo.com; mafarajzadeh@tabrizu.ac.ir

UP	Unadsorbed percent
RR	Relative recovery
PrA	Propylamine
sec-BuA	sec-Butylamine
BuA	Butylamine
PeA	Pentylamine
BeA	Benzylamine

Primary aliphatic amines (PAAs) are the organic compounds characterized by the presence of an -NH_2 functional group attached to a saturated carbon chain[1,2]. These compounds play a crucial role in various chemical reactions and serve as fundamental building blocks in the synthesis of pharmaceuticals, agrochemicals, and other essential organic materials[3]. PAAs are widely employed across the chemical, pharmaceutical, petrochemical, and textile industries. However, inadequate wastewater treatment in these industries can lead to the release of PAAs into the environment, adversely affecting water and soil quality. PAAs are recognized as toxic pollutants that pose serious risks to ecosystems[4–8]. Moreover, prolonged exposure to these amines can have severe health implications, including neurological and pulmonary disorders[9,10]. Therefore, the accurate identification and quantification of PAAs are essential for assessing environmental pollution and potential health hazards[11].

To precisely determine PAAs, various analytical techniques have been developed, including gas chromatography (GC)[12–14], high-performance liquid chromatography[11,15,16], and spectrofluorimetry[17]. However, the analysis of PAAs in aqueous samples is challenging due to their low concentrations and complex sample matrices. To enhance sensitivity and reduce matrix effects, extraction and preconcentration techniques are often employed. Among these techniques, liquid-liquid extraction[18] and solid phase extraction (SPE)[19] are widely utilized. However, both methods present limitations, such as excessive consumption of organic solvents, high costs, and time-consuming procedures. Additionally, SPE may suffer from cartridge blockage and memory effects[20]. Microextraction techniques have been introduced to overcome these limitations. In single-drop microextraction, a single droplet of an extractant is used to isolate analytes; however, this method faces the issues such as instability of the organic drop under rapid stirring and prolonged extraction times[20]. Similarly, in hollow fiber-liquid phase microextraction, an extractant droplet is housed inside a hollow fiber, but this technique often suffers from low efficiency and long extraction times[21]. Solid-phase microextraction is a solvent-free approach, yet it is typically associated with high costs and limited extraction efficiency[22–24]. Dispersive liquid-liquid microextraction offers a rapid and efficient alternative, in which an extractant is fully dispersed within an aqueous sample, enhancing extraction efficiency[25,26]. However, this method relies on a disperser solvent, which poses a significant limitation. Due to its semi-polar nature, the disperser solvent decreases the polarity of the aqueous phase, increasing the solubility of analytes in water and thereby reducing their tendency to be extracted into the organic phase. Furthermore, rapid injection of the extraction solvent can lead to the loss of certain analytes, particularly volatile compounds, during sample preparation[27]. Vortex-assisted liquid-liquid microextraction (VALLME) overcomes this limitation by employing vortex agitation to disperse the extraction solvent within the sample solution, eliminating the need for a disperser solvent. This method not only reduces costs but also minimizes the loss of volatile analytes[28,29].

The extraction of PAAs from aqueous samples is particularly challenging due to their high polarity. Additionally, in GC analysis, PAAs may interact with the stationary phase, causing peak tailing and unreliable results. To mitigate these issues, derivatization reactions are commonly employed[30]. Several derivatization agents have been used for PAAs, including silylating agents[31], acylating agents[32], alkylating agents[33], and carbamates[34]. Each of them offers distinct advantages in terms of efficiency, specificity, and nature of the resulting derivatives. Alkyl chloroformates, particularly butyl chloroformate (BCF), are suitable derivatization agents for PAAs due to their ability to form stable alkyl carbamate derivatives, which improve chromatographic properties[35]. Under alkaline conditions, the derivatization rate increases, leading to the formation of more stable and efficient derivatives[34].

To ensure the accurate quantification of PAAs in complex real-world samples, it is essential to minimize or eliminate matrix effects. Dispersive micro-solid phase extraction (DμSPE) represents a promising approach, in which finely dispersed adsorbent particles enhance analytes interaction and extraction efficiency[36]. The effectiveness of this technique depends on the specific adsorbent employed, which should be capable of selectively not adsorbing PAAs while eliminating matrix interferences. Given the structure and pH sensitivity of PAAs, an adsorbent that functions within an appropriate pH range is required to optimize extraction while minimizing the matrix effect.

This study was conducted in two parts: passivation of adsorbent in elimination of PAAs, and simultaneous extraction and derivatization of PAAs during VALLME. In the first step, the DμSPE conditions were optimized using iron oxide modified with mercaptoacetic acid (MAA@Fe_3O_4) as the adsorbent, aiming to reduce matrix effects while preserving PAAs in solution. In the second step, the VALLME method was applied for the concurrent extraction and derivatization of PAAs. BCF was utilized as the derivatization agent, allowing for the efficient conversion of PAAs into carbamate derivatives and their subsequent extraction. This method demonstrates great potential for PAAs analysis due to its utilization of μL-scale extractant and derivatization reagents, eco-friendly adsorbent, and enhanced extraction efficiency.

Experimental

Chemicals and solutions

The utilized PAAs included propylamine (PrA), butylamine (BuA) (purchased from Fluka, Bosch, Switzerland), pentylamine (PeA), benzylamine (BeA), and *sec*-butylamine (*sec*-BuA) (obtained from Merck, Darmstadt, Germany). A standard solution of PAAs with a concentration of 500 mg L^{-1} (of each analyte) was prepared

in methanol. To prepare the daily standard solutions, it was diluted using deionized water (obtained from Ghazi Company, Tabriz, Iran). For adsorbent synthesis process, iron sulfate heptahydrate ($FeSO_4.7H_2O$) 99.5%, mercaptoacetic acid (MAA) 98%, concentrated ammonia solution (25%, *w/w*), ethanol 99.8%, and iron chloride hexahydrate ($FeCl_3.6H_2O$) 98.5% (all purchased from Merck) were used. To optimize the ionic strength, sodium sulfate 99%, potassium chloride 99.9%, sodium chloride 99% (purchased from Merck), to adjust pH of the aqueous phase, sodium hydroxide 99% and hydrochloric acid (37%, *w/w*) (purchased from Fluka), and to prevent precipitation of possible cations in samples in alkaline media disodium ethylenediaminetetraacetic acid (EDTA) (obtained from Merck) were utilized. In this work extraction solvents including 1,1,1-trichloroethane (1,1,1-TCE) 99.7%, 1,2-dibromoethane (1,2-DBE) 98%, chloroform ($CHCl_3$) 99%, and 1,1,2-trichloroethane(1,1,2-TCE) 99.5% (obtained from Johnson, Beerse, Belgium) were utilized.

Samples

Three skin moisturizers were purchased from a cosmetic store (Tabriz, Iran). All samples were placed in contact with the adsorbent according to the DμSPE method to eliminate or decrease the matrix effect (without dilution). Then, the supernatant was subjected to the simultaneous derivatization and extraction of PAAs in VALLME method. It should be noted that before adjusting pH at 10, EDTA (10 mg) was added to 5 mL of each sample.

Apparatus

A GC equipped with flame ionization detector (FID) model 2014 (manufactured by Shimadzu, Kyoto, Japan) was used to study the matrix effect of real samples before and after contact with the adsorbent, and to separate, identify, and quantify the derivatized PAAs. The instrument was equipped with a split/splitless injector that was set in a splitless/split mode (split time 1 min and split ratio 1:10) thermostated at 300 °C. The FID temperature was set at 300 °C. A capillary column (dimethyl: diphenylpolysiloxane 95:5) with a length of 30 m, inner diameter of 0.25 mm, and a stationary phase film thickness of 0.25 µm (Restex, Center, PA, USA) was used for the separation and detection of PAAs. The initial temperature of column oven was adjusted at 60 °C and maintained at this temperature for 2 min. Then it was increased to 200 °C with a ramp of 10 °C min^{-1} and maintained at this temperature for 2 min. The carrier gas utilized was helium (99.999%, Crewe Bay, Dubai, United Arab Emirates) which was introduced into the GC at a linear velocity of 30 cm s^{-1}. The fuel used in the FID was hydrogen supplied by a hydrogen generator (OPGU 1500 S, Shimadzu, Kyoto, Japan) with a flow rate of 30 mL min^{-1}. Also, the oxidant used in FID was air, which entered the FID chamber with a flow rate of 300 mL min^{-1}. Drying the synthesized MAA@Fe_3O_4 was done using an oven (Heraeus UT 12, Hanau, Germany). A vortex (Labinco L46 vortex mixer, Breda, the Netherlands) was utilized to establish sufficient contact between the analytes and adsorbent. After derivatization and extraction, a centrifuge (Hettich D7200, Kitchener, Germany) was used to facilitate separation of organic and aqueous phases. pH of samples was adjusted before the contact of the analytes with the adsorbent and before derivatization and extraction by employing a pH meter (Metrohm 654, Herisau, Switzerland). To identify the adsorbent morphology and assess its composition, scanning electron microscopy (SEM) and energy diffraction X-ray (EDX) analysis were employed using a Mira 3 microscope (Tescan Mira 3, Brno, Czech Republic). Fourier transform infrared (FTIR) (Bruker, Billerica, MA, USA) and X-ray diffraction (XRD) (Siemens D500 diffractometer AG, Karlsruhe, Germany) analyses were performed to authenticate the synthesis and formation of the desired bonds. To verify the magnetic characteristics of the adsorbent, vibrating sample magnetometry (VSM) (MDKB, Magnetic DaneshPajoh Kashan Co. Kashan, Iran) was conducted, and for assessing the surface area and pores size, Brunauer-Emmett-Teller (BET) analysis was performed using a BELSORP-mini-instrument (MicrotracBEL Corp, Osaka, Japan). Thermogravimetric analysis (TGA) was carried out using a Linseis L81-A 1750 (Robbinsville, USA) under 5 mL min^{-1} nitrogen flow rate. The experiment was conducted over a temperature range of 30–600 °C with a controlled heating rate of 10 °C min^{-1}.

Synthesis of MAA@Fe3O4

Synthesis of magnetic adsorbent functionalized with MAA included two steps. The first step was the synthesis of Fe_3O_4 particles as described in our previous work[37]. The second step was functionalizing MAA on Fe_3O_4 particles[38]. For this purpose, 0.267 g of MAA was dissolved in 100 mL of ethanol and then 0.5 g of Fe_3O_4 particles were added into it. The resulting mixture was stirred on a stirrer for 24 h, and then MAA@Fe_3O_4 particles were collected from the reaction mixture using an external magnetic field and washed with a 1:1 mixture of ethanol and water (several times). Finally, MAA@Fe_3O_4 microspheres were dried in an oven at 50 °C for 3 h under vacuum conditions.

Clean up and derivatization/ extraction procedures

DμSPE step

Five milliliters of real sample or deionized water (spiked with the analytes at 500 mg L^{-1} of each amine) was poured into a 10-mL conical bottom glass test tube, and pH of solution was adjusted at 10 using 0.1 M NaOH solution. Sodium chloride (0.375 g) was added to adjust the ionic strength along with 10 mg of EDTA to prevent unexpected precipitates formation. Finally, 20 mg of MAA@Fe_3O_4 was added to the solution and then vortexed for 3 min to establish adequate contact between the analytes and MAA@Fe_3O_4 particles. It should be noted that to prevent the escape of PAAs, everything that was added to the glass test tube immediately and the cap was put on it. An external magnetic field was used to easily separate the adsorbent particles from the solution in a short time. Then the supernatant was transferred into another glass test tube.

VALLME step

Due to the acidity of the adsorbent, after the contact of the aqueous solution with the adsorbent, its pH decreased. As mentioned in the introduction section, the suitable pH for the derivatization of PAAs is an alkaline medium.

Therefore, first, the pH of the supernatant (obtained from the DμSPE step) was checked and re-adjusted at pH 10. Then 5 μL of BCF was mixed with 15 μL of 1,1,2-TCE inside a 1-mL conical bottom vial, and then slowly introduced into the aqueous solution by a 50-μL syringe. The cap was immediately placed and vortexed for 5 min to perform derivatization and extraction. To separate the phases and settle down the extractive phase, it was centrifuged for 3 min with a speed of 4000 rpm. Finally, 1 μL of the settled phase (10 ± 0.5 μL) was injected into GC-FID. The schematic of whole process is shown in Fig. 1.

Calculations

Enrichment factor (EF) is an indication of the extent of analytes preconcentration (Eq. 1). Extraction recovery (ER%) serves as an indicator of how effectively analytes are extracted from an aqueous phase into the organic phase (Eq. 2). Unadsorbed percent (UP%) of the analyte indicates the percentage of analyte that is not adsorbed by the adsorbent (Eq. 3). This equation is used exclusively in the DμSPE stage. The high value of this parameter is favorite in this study. Relative recovery (RR%) is a criterion for evaluating the effectiveness of the proposed method, indicating whether complex matrices can diminish the method's efficiency (Eq. 4).

$$EF = \frac{C_{sed}}{C_0} \tag{1}$$

$$ER\% = \frac{n_{sed}}{n_0} \times 100 = \frac{C_{sed} \times V_{sed}}{C_0 \times V_0} \times 100 = EF \times \frac{V_{sed}}{V_0} \times 100 \tag{2}$$

In these equations, C_{sed} represents concentration of analyte in organic phase, C_0 indicates the initial concentration of analyte in aqueous solution, n_{sed} denotes the number of moles of analyte in the organic phase, n_0 signifies the number of moles of analyte in initial aqueous phase, V_{sed} refers to the volume of the sedimented organic phase, and V_0 represents the volume of the aqueous phase.

$$UP\% = 100 - \left[\left(\frac{C_{sed_1} - C_{sed_2}}{C_{sed_1}}\right) \times 100\right] \tag{3}$$

In this equation, C_{sed_1} represents the concentration of analyte extracted directly from the aqueous solution without contacting with the adsorbent, while C_{sed_2} denotes the concentration of analyte extracted from the supernatant solution after contacting with the adsorbent. In this equation, if PAAs are entirely adsorbed, no PAAs will be present in the supernatant solution, making the value of C_{sed_2} equal to 0, resulting in UP% being 0. If PAAs are not adsorbed at all, PAAs will be found in the supernatant solution and C_{sed_2} will be equal to C_{sed_1}, making UP% = 100. Therefore, in the intermediate states, the value of UP% varies from 0 to 100.

$$RR\% = \frac{C_{total} - C_{real}}{C_{added}} \times 100 \tag{4}$$

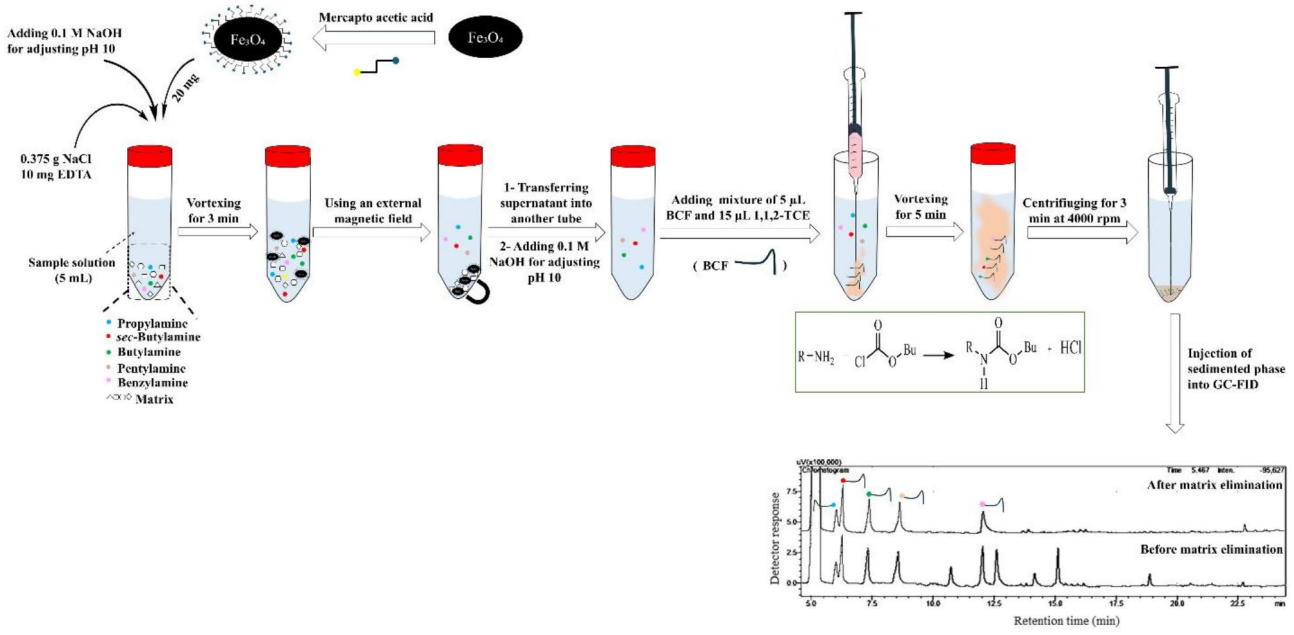

Fig. 1. Schematic of whole process of clean up and derivatization/extraction procedures.

In this equation, C_{real} is concentration of the analyte in real sample, C_{added} is the spiked concentration of the analyte to the real sample, and C_{total} is total concentration of the analyte in the real sample after spiking.

Results and discussion

Characterization of MAA@Fe3O4

SEM is a powerful tool for studying the surface of materials with very high magnification. Through SEM images, surface morphology, particles size, size distribution, and other surface characteristics of materials can be examined. Figure 2a shows the particles have an irregular and sometimes granular morphology. Their size is in the range of 30–50 nm, and the distribution of particles size is relatively uniform.

EDX is the technique used to determine the elemental composition of solid samples. The spectrum reported in Fig. 2b confirms the presence of iron, carbon, oxygen, and sulfur in the adsorbent composition. The presence of iron and carbon, respectively, indicates the magnetic phase and the presence of organic substance in the absorbent structure. The peak related to sulfur confirms the presence of MAA in the absorbent structure. It should be noted that there is a specific peak at around 2.3 Kev, which is related to the gold coating used to increase the electrical conductivity of the sample.

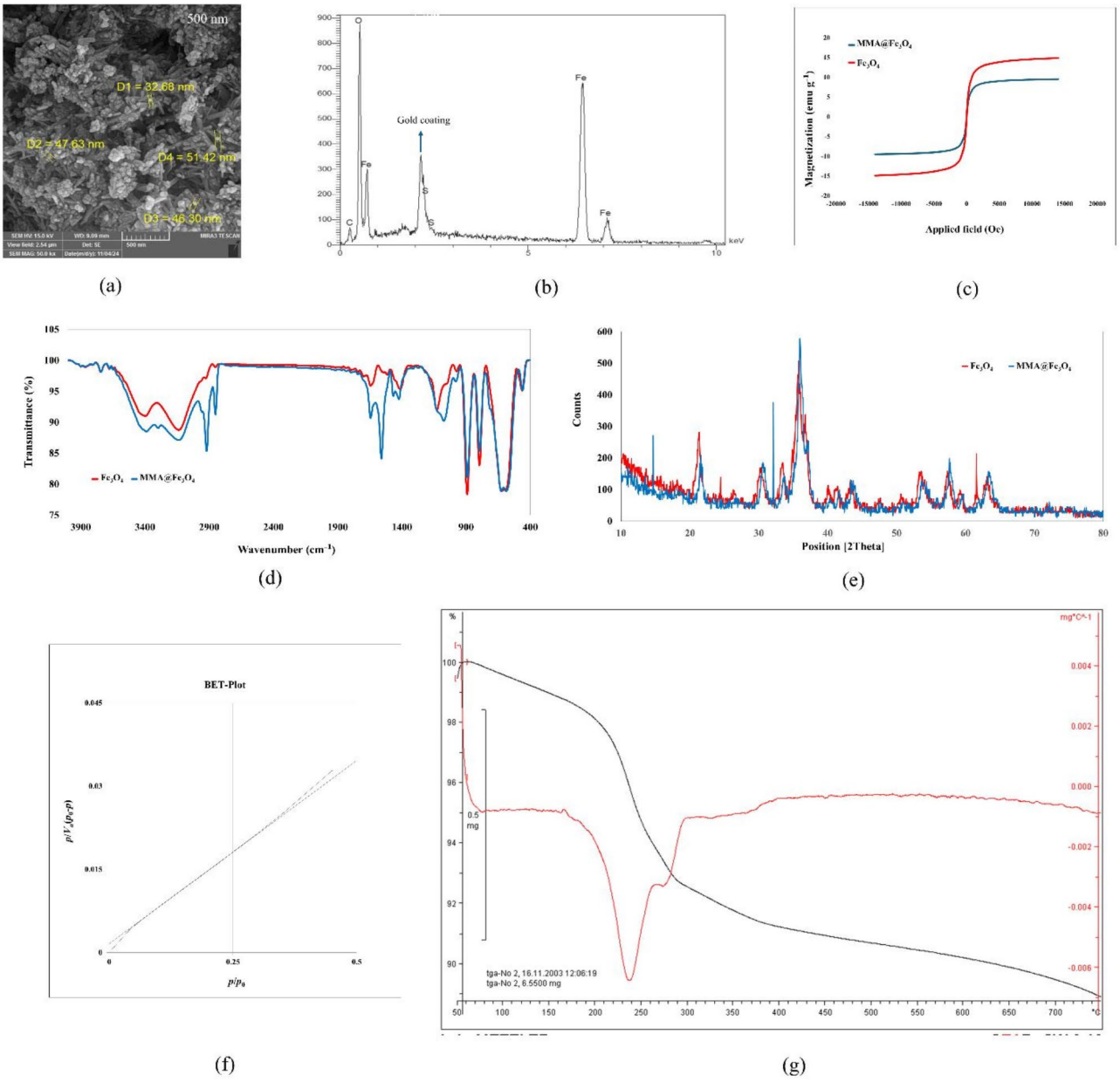

Fig. 2. SEM images of MAA@Fe_3O_4 (**a**), EDX spectrum of MAA@Fe_3O_4 (**b**), VSM curve of Fe_3O_4 and MAA@Fe_3O_4 (**c**), FTIR spectra of Fe_3O_4 and MAA@Fe_3O_4 (**d**), XRD pattern of Fe_3O_4 and MAA@Fe_3O_4 (**e**), BET curve of MAA@Fe_3O_4 (**f**), and TGA curve of the MAA@Fe_3O_4.

VSM is an appropriate technique for assessing the magnetic characteristics of materials. As illustrated in Fig. 2c, the hysteresis curve of MAA@Fe_3O_4 demonstrates its ferromagnetic or superparamagnetic characteristics. At 300 K, the saturation magnetization of Fe_3O_4 is measured at 14.82 emu g^{-1}, while that of MAA@Fe_3O_4 is 9.52 emu g^{-1}. Consequently, it can be inferred that the coating MAA on Fe_3O_4 nanoparticles decreases their magnetization, and this alteration arises from the interactions between Fe_3O_4 nanoparticles and MAA, leading to magnetic anisotropy.

FTIR is an effective method for identifying functional groups and chemical bonds in different substances. In this study, FTIR spectra of Fe_3O_4 and MAA@Fe_3O_4 (Fig. 2d), were examined to assess the influence of the coating on the sorbent structure and composition. The main peak occurring around 625 cm^{-1} corresponds to the stretching vibration of the Fe-O bond within Fe_3O_4 structure. This peak verifies the existence of Fe_3O_4 phase in the sorbent. Wide peaks at approximately 3395 cm^{-1} and a faint peak near 1643 cm^{-1} correspond to water molecules that are adsorbed on the surface of Fe_3O_4 nanoparticles. To examine the spectrum of MAA@Fe_3O_4 in greater details, we needed to identify the alterations that took place in comparison to the spectrum of Fe_3O_4. These alterations may signify the existence of functional groups of MAA on the nanoparticle surface. The wide peak associated with the stretching vibration of O-H bond at 3395 cm^{-1} is more intense in the MAA@Fe_3O_4 spectrum compared to the Fe_3O_4 spectrum. This is attributed to the existence of carboxylic acid groups (-COOH) in MAA. The peak associated with the stretching vibration of the carbonyl bond (C = O) within the carboxylic acid group is seen in the range of 1559 cm^{-1}. The peak related to the stretching vibration of C-S bond is seen at around 587 cm^{-1}. Based on the observations recorded, it can be inferred that the functionalization procedure has been effectively achieved and the MAA is bonded onto the Fe_3O_4 nanoparticle surface.

XRD is one of the suitable tools for identifying crystalline phases and structural changes in materials. To confirm the success of the MAA@Fe_3O_4 synthesis and investigate the binding MAA, XRD patterns for Fe_3O_4 and MAA@Fe_3O_4 were prepared and are shown in Fig. 2e. These patterns were recorded in the range of 2θ between 10 and 80°. In the spectrum of Fe_3O_4, the specific peaks of the spinel structure in the crystal planes of (111), (220), (311), (400), (422), (511), and (440) at the 2θ values equal to 18, 30.1, 35.5, 43.1, 53.4, 57.3, and 62.5, respectively, are observed. These peaks are still present in the spectrum of MAA@Fe_3O_4, but a significant decrease in their intensity is seen, especially at 35.5 and 62.5°. This decrease in intensity indicates the surface coating of particles by MAA. Also, the slight increase in baseline at low 2θ values confirms the presence of organic groups. The changes observed in the XRD spectrum confirm that MAA is successfully functionalized on the surface of Fe_3O_4 particles.

BET analysis determines the specific surface area, cumulative pores volume, and pores size distribution of porous materials by measuring the amount of nitrogen adsorption at a constant temperature of liquid nitrogen. Figure 2f shows the nitrogen adsorption isotherm of the adsorbent based on the BET method. The results of this analysis show that the specific surface area of the absorbent is equal to 64.275 m^2 g^{-1}, its cumulative pores volume is 0.3527 cm^3 g^{-1}, and the average diameter of its pores is 21.949 nm. The high values of the specific surface area and cumulative pores volume indicate the presence of active surface and high porosity in the absorbent structure, which are very favorable for adsorption and catalytic applications. Also, the average pores diameter obtained shows that the adsorbent has pores in mesoporous range.

To further investigate the thermal stability of the adsorbent, TGA was performed. The TGA was conducted under a controlled heating rate and an inert atmosphere to evaluate the decomposition profile of the adsorbent. The weight loss at different temperature ranges was analyzed to identify the thermal behavior of the MAA@Fe_3O_4 and its structural stability at elevated temperatures. The TGA curve revealed a slight weight loss up to 200 °C, attributed to removing adsorbed water and residual solvents. A more significant reduction between 200 and 350 °C indicated the decomposition of organic groups of the adsorbent. Based on these findings, the adsorbent remains structurally intact below 200 °C, making it the optimal temperature range for its application. The detailed thermal degradation profile is presented in Fig. 2g.

Optimization of parameters in DμSPE-VALLME

Aqueous solution pH in DμSPE stage

Considering that MAA has a carboxylic acid group, it can be expected that pKa of the MMA attaches to Fe_3O_4 to be in the range of pK_a of common carboxylic acids (between 4 and 5). The adsorbent at pH lower and higher than this range is in the forms of R-COOH and $R\text{-}COO^-$, respectively. In addition, considering that the pK_a of ammonium forms of the PAAs is in the range 9.3–10.7, these compounds are in the forms of $R\text{-}NH_3^+$ and $R\text{-}NH_2$ at the pHs lower and higher than this range, respectively. At pH below 4, both adsorbent and PAAs are in the protonated forms and have no electrostatic attraction. At pH above 9, the adsorbent and PAAs are in $R\text{-}COO^-$ and $R\text{-}NH_2$ forms, respectively, so electrostatic attraction between the adsorbent and the PAAs does not occur. In the pHs between 4 and 9, the adsorbent and PAAs are in the forms of $\text{-}COO^-$ and $R\text{-}NH_3^+$, respectively, and the PAAs are electrostatically adsorbed by the adsorbent. To examine the influence of pH on PAAs adsorption, the pH values of 1, 3, 7, 10, and 13 were investigated and assessed according to the UP% criteria (Fig. 3). As expected, the lowest UP% value or highest adsorbed value is related to neutral pH, which indicates the electrostatic attraction between the adsorbent and PAAs. At pH 3, the level of PAAs adsorption is lower than that of pH 7. This is likely because, at this pH, some parts of the adsorbent exist as R-COOH and another part as $R\text{-}COO^-$, allowing it to adsorb some portions of the PAAs electrostatically. At pH 1, the quantity of UP% is risen, due to decreasing $R\text{-}COO^-$ form in this pH. At pHs 10 and 13, all analytes show the highest UP% values (lowest adsorbed values). Likely, PAAs exist mainly in their $R\text{-}NH_2$ forms at these pHs, which prevent them from interacting electrostatically with the adsorbent. The high UP% values at pH 13 can also be attributed to the increased probability of the adsorbent degradation. Once the adsorbent is degraded, the adsorption is disturbed. It is important to mention that at pH 13, it was visually observed that the adsorbent amount was reduced probably due to its degradation.

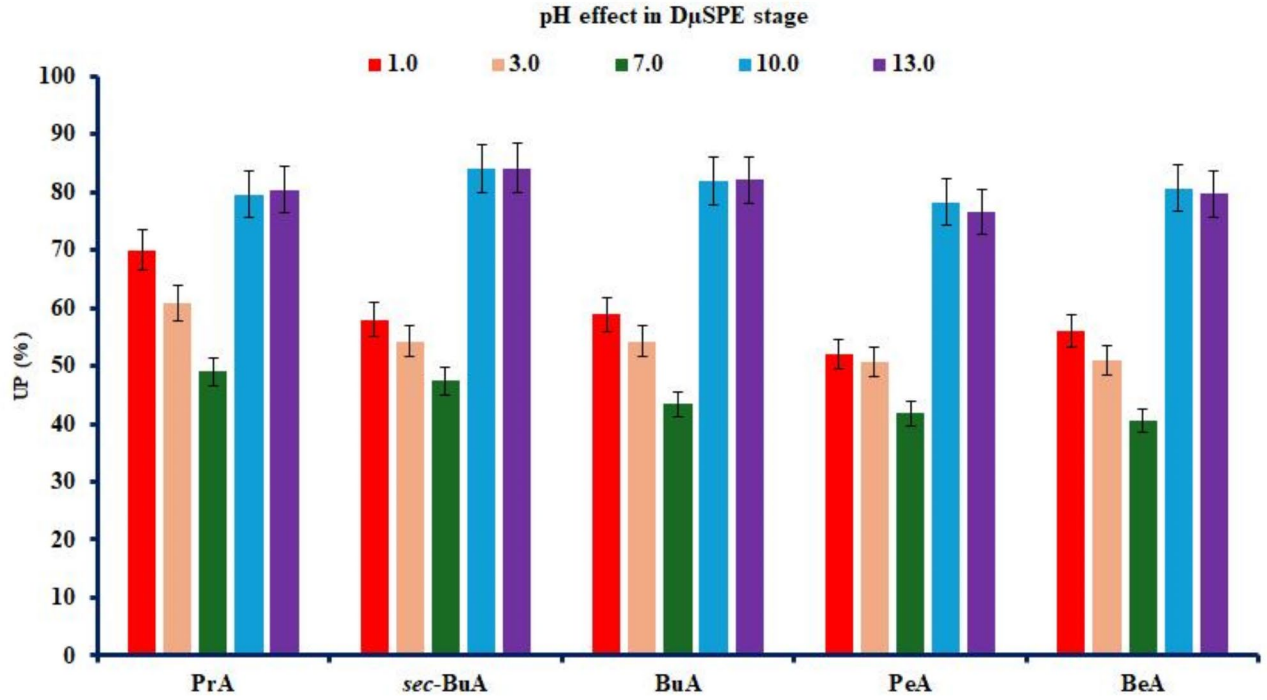

Fig. 3. Optimization of pH in DμSPE stage. DμSPE conditions: aqueous solution, 5 mL of deionized water spiked with 500 μg L^{-1} of each analyte in which 0.375 g NaCl was dissolved; adsorbent amount, 15 mg; and vortexing time, 5 min. VALLME conditions: aqueous phase, the supernatant separated from the previous step, without pH adjusting; extraction solvent, 1,1,2-TCE with a volume of 15 μL; derivatization agent, BCF with a volume of 5 μL; vortexing time, 5 min, and centrifugation rate and time, 5000 rpm and 5 min, respectively. Error bars depict the minimum and maximum values of three repeated determinations.

Therefore, pH 10 was selected for the further studies.

MAA@Fe3O4 weight

In this section, several factors should be considered to select the optimal adsorbent weight: the method's efficiency, cost-effectiveness, the elimination or decreasing matrix effect, and the prevention of PAAs adsorption by the sorbent. The values of 3, 5, 10, 15, 20, 25, and 30 mg adsorbent were examined and evaluated based on the UP% criteria to optimize the adsorbent weight. According to the reported findings (Fig. 4), the UP% values remain constant in the weights ≤ 20 mg. Increasing the adsorbent weight beyond 20 mg has led to a reduction in UP%. The objective of this study is to eliminate or reduce the sample matrix effect while preserving the presence of PAAs in the samples; consequently, it is imperative to determine the maximum adsorbent weight that does not eliminate PAAs. Accordingly, 20 mg of the adsorbent was selected as the ideal weight that suits the aims of this study for the future optimizations.

Ionic strength study

The adjusting the ionic strength of an aqueous solution is accomplished through addition of a salt. The process of salt addition can have two distinct outcomes. The introduction of salt into the aqueous solution decreases the solubility of PAAs, which enhances their adsorption (thereby reducing UP% values), a phenomenon referred to "salting-out" effect. Conversely, the addition of salt may lead to an increase in viscosity of the aqueous solution, a reduction in the adsorption of PAAs (increasing UP% values), known as the "salting-in" effect. According to the procedure stated in Sect. 2.5, the aqueous solution containing PAAs, after contact with the adsorbent, was subjected to simultaneous extraction and derivatization conditions. Therefore, the effect of salt addition can be effective in both DμSPE and VALLME steps. To investigate this parameter, three salts consisting of sodium chloride, sodium sulfate, and potassium chloride with a concentration of 1 M as well as without salt addition were utilized. It should be noted that the UP% and ER% criteria during the DμSPE and VALLME stages, respectively, were employed to assess the effect of salt addition. As reported in Fig. 5a, in the DμSPE stage, sodium chloride and sodium sulfate have the highest and lowest UP% values, respectively. Sodium sulfate increases the adsorption of PAAs because it induces higher ionic strength than other salts. On the other hand, sodium chloride reduces the adsorption of PAAs due to its higher viscosity than saltless case. As reported in Fig. 5b, sodium chloride has the highest ER% in the VALLME stage. Therefore, NaCl was selected as the optimal salt in both stages.

Afterward, it is necessary to optimize the concentration of sodium chloride salt. Different concentrations from 5 to 30% *(w/v)* were evaluated using the proposed method. According to Fig. S1a, it is observed that with the increase of sodium chloride concentration up to 7.5% *(w/v)*, the viscosity of the solution increases and the

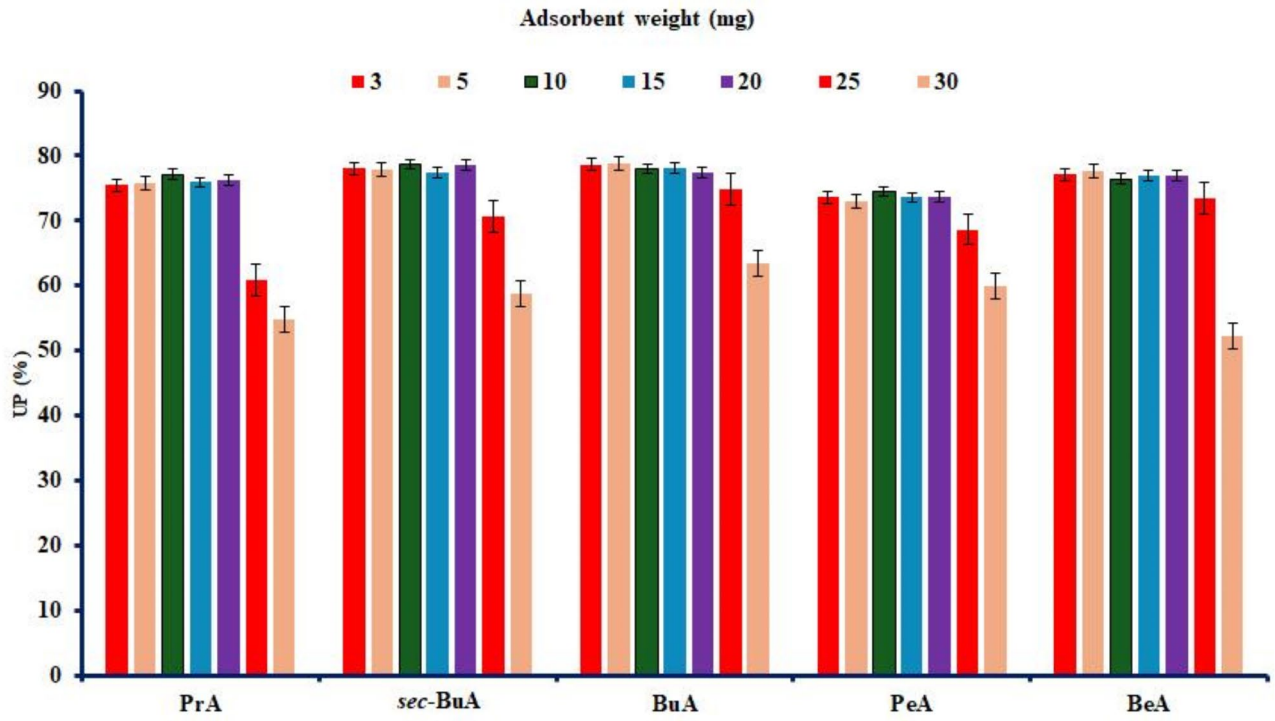

Fig. 4. Optimization of adsorbent amount. Experimental conditions were identical to those implemented in Fig. 3, except for adjusting pH in DμSPE step at 10.

adsorption of PAAs decreases, after that, it has no effect on the adsorption. Figure S1b also shows that in the concentrations less than 7.5% *(w/v)*, "salting-out" effect doesn't work well, and in the concentrations higher than 7.5% *(w/v)*, the ERs% decrease gradually due to the increase in viscosity of solution. Therefore, sodium chloride 7.5% *(w/v)* was used as the optimal salt in the next optimization steps.

Vortexing time in DμSPE stage

Vortex operation is another key parameter in the adsorption process. Therefore, it is necessary to optimize the vortexing time. To accurately adjust the duration of vortexing, 3, 5, 7, and 9 min were selected, and Ups% of the analytes were evaluated. The findings show that the UP% values in the examined times are not significantly different (Fig. S2), and 3 min vortexing was chosen for the further tests.

Derivatization agent volume

BCF serves as an appropriate derivatization agent for PAAs in alkaline conditions. It was determined that optimizing BCF volume is essential for achieving high derivatization. Therefore, volumes of 3, 5, 7, 9, and 11 μL of BCF were examined and compared based on ER% values. As shown in Fig. S3, BCF volumes below and above 5 μL result in reduced derivatization and decreased ERs%. It is clear that derivatization is not fully achieved in the volumes under 5 μL. In the volumes exceeding 5 μL, BCF is hydrolyzed and pH of solution decreases. It leads to incomplete derivatization of amines. Thus, 5 μL of BCF was utilized as the ideal volume of the derivatizing agent for the subsequent optimization steps.

Study of pH in VALLME stage

Derivatization of PAAs is only possible in alkaline media because PAAs in acidic pHs are as R-NH3$^+$ form, which cannot be derivatized. As mentioned in the DμSPE section, pH 10 was chosen as the optimal pH of the aqueous phase. It has been observed that after adding adsorbent and EDTA, pH of the aqueous solution decreased from 10 to 8.5-9.0, which reduced the possibility of PAAs derivatization. For this reason, it is necessary to re-optimize the pH of the aqueous phase. In this regard, pH 8, 9, 10, and 11 were compared based on ER% criteria. Based on the reported findings (Fig. S4), low ERs% are achieved at pH 8, likely because some PAAs of the portions exist in R-NH_3^+ form, rendering their derivatization unfeasible. According to the pK_a values of PAAs, at pH 10, most portions of the PAAs are in R-NH_2 form, so derivatization and ER% values are increased. At pH 11, due to the hydrolysis of BCF, ER% values are decreased. Therefore, pH 10 was chosen as the optimal pH in this step.

Type and volume of extraction solvent

How to extract the derivatized PAAs depends on choosing a suitable extraction solvent. This extractant should have the following characteristics: immiscibility and higher density than deionized water, no reaction with BCF, and high ability to dissolve the derivatized PAAs. To determine the appropriate extraction solvent, ER% values were compared for 1,1,2-TCE, 1,1,1-TCE, 1,2-DBE, and $CHCl_3$ solvents. Respectively 15, 16, 15, and 26 μL of

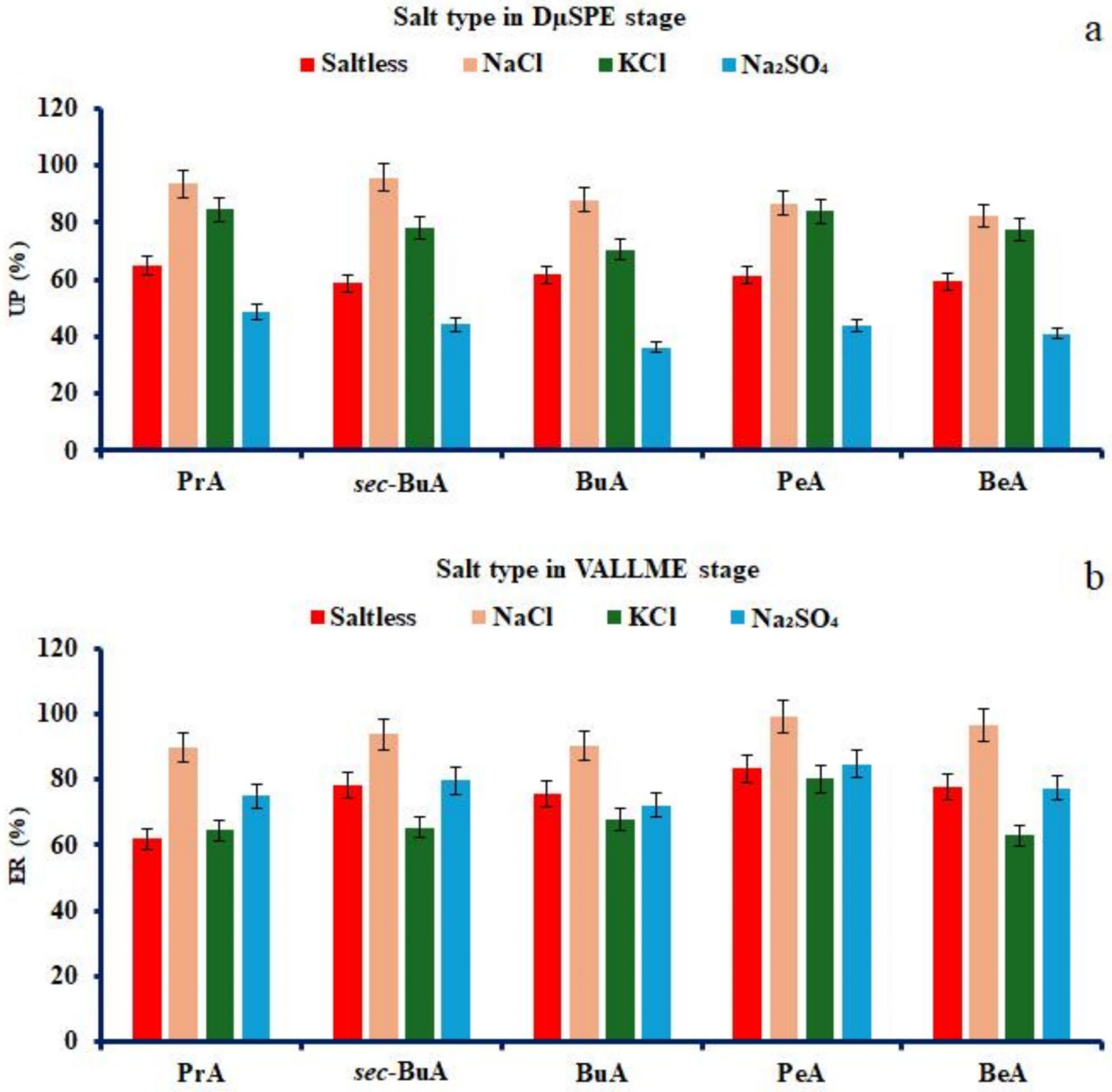

Fig. 5. Influence of ionic strength on UP% and ER% values of the analytes in DμSPE (**a**) and VALLME (**b**) steps. Experimental conditions were the same as those shown in Fig. 4, except that the adsorbent weight utilized was 20 mg.

the mentioned solvents were utilized to achieve a specific organic phase volume (10 ± 0.5 µL). Figure 6 shows that 1,1,2-TCE has the highest ER% values for PAAs. The reason for this is high ability of 1,1,2-TCE to dissolve analytes compared to the other solvents, which led to more PAA derivatives being extracted.

In the next step, 1,1,2-TCE volume was optimized. At this stage, the volumes of 15, 20, 25, and 30 µL were evaluated using EF values. The volumes of the sedimented phase when using the mentioned volumes of the solvent were 10, 15, 21, and 27 µL, respectively. According to the results reported in Fig. S5, increasing the extractant volume leads to a decrease in EFs, which is attributed to the dilution phenomenon. Therefore, 15 µL of 1,1,2-TCE was selected for the PAAs extraction.

Vortexing time in VALLME step

To complete the extraction process, after adding BCF and 1,1,2-TCE, the mixture must be vortexed. The duration of this process is one of the most important parameters of extraction. To optimize the vortexing time, 1, 3, 5, 7, and 9 min were evaluated and compared based on ER% values. As reported in Fig. S6, the duration of 5 min has the highest ER% values. At low vortexing times, sufficient opportunity for the simultaneous extraction and derivatization of PAAs is not provided, therefore ER% values are low. At high vortexing times,

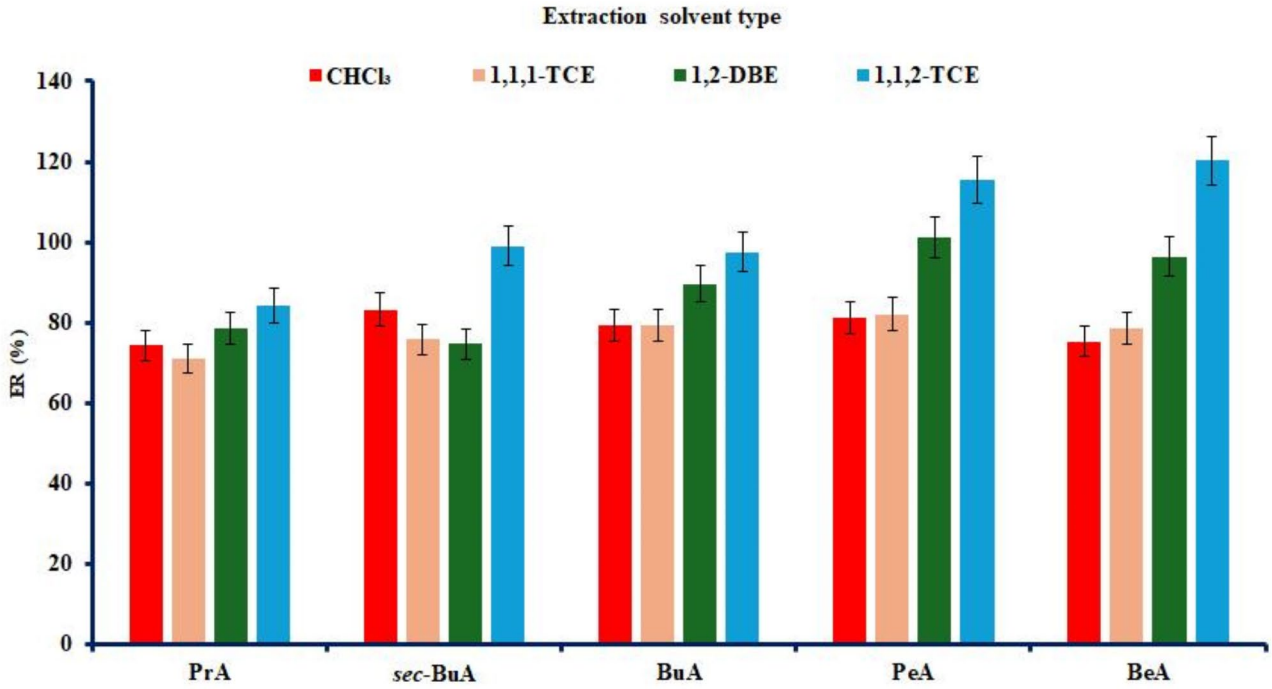

Fig. 6. Selection of extraction solvent type. Experimental conditions correspond to those shown in Fig. 5, except for adjusting pH in VALLME at 10, and the vortexing time at 3 min.

due to the disruption of the balance between derivatization and providing sufficient time for back extraction, the amount of ERs% decreases. Therefore, a duration of 5 min was chosen as the optimal vortexing time for the next optimizations.

Centrifugation operation

Centrifugation operation is one of the necessary steps in the extraction process, which is utilized for phases separation. Figures S7a, and S7b show the effect of time (3, 5, 7, and 9 min) and centrifugation rate (4000, 5000, 6000, and 7000 rpm) in the extraction process. As can be seen from Fig. S7a, with the increase in centrifugation time, there is a noticeable decrease in ER% values, which can be attributed to the heat generated in the centrifuge, which leads to the back extraction of the derivatized PAAs. As reported in Fig. S7b, centrifugation rate has no significant effect on ER% values. Therefore, in the operation of the centrifugation, the duration of 3 min and the rate of 4000 rpm were chosen as optimal values.

Reusability of adsorbent

The ability of the adsorbent to eliminate or decrease matrix effect in skin moisturizers while maintaining PAAs in solution was assessed, revealing the absence of a memory effect. Following the adsorption of the matrix, components the adsorbent was rinsed with a mixture of *iso*-propanol and deionized water (1:3, v/v) to desorb the adsorbed compounds onto the sorbent surface. The method's efficiency for matrix effect elimination was validated over 5 successive cycles using the same adsorbent, with RSD ≤ 8%.

Chemical stability of adsorbent

To evaluate the chemical stability of the adsorbent, it was treated at the pHs 1, 3, 7, 10, and 13. In each case, the adsorbent was exposed to ultrasonic waves for 30 min. After treatment, it was separated from the solution and washed with deionized water. The adsorbents were then analyzed using a DμSPE-VALLME method for eliminating the matrix effects of skin moisturizers and simultaneously derivatizing and extracting primary aliphatic amines used in the samples. The results showed that at pH 3, 7, and 10, the adsorbent remained completely stable, with its performance matching that of an untreated adsorbent. However, at pH 1, the adsorbent likely led to the partial degradation, releasing Fe^{2+} and Fe^{3+} ions into the medium. This resulted in a 20% reduction in the adsorbent efficiency. At pH 13, the adsorbent experienced severe degradation, with a noticeable decrease in the amount of material, even visibly. This significant deterioration could be attributed to 1: Surface oxidation of Fe_3O_4, leading to its transformation into other iron oxide phases, 2: Formation of the soluble complex $[Fe(OH)_4]^-$ from Fe^{3+} in the highly alkaline environment, 3: Conversion of thiol (-SH) groups to thiolate ($-S^-$), weakening the Fe-S bond, 4: Detachment of the MAA layer from the Fe_3O_4 surface. These findings indicate that the adsorbent exhibits high chemical stability in the pH range of 3–10. However, in strongly acidic (pH 1) and highly alkaline (pH 13) conditions, it undergoes structural degradation, leading to reduced performance.

Method validation

In this section, various analytical parameters were assessed and the data are presented in Table 1 to validate the approach under study. UP% is an important parameter in the DμSPE section that evaluates the efficiency of the adsorbent. The UP% values obtained for PAAs were in the range of 92–97%. ER% and EF are two effective parameters to evaluate the extraction method, which were in the ranges of 84–105% and 420–525, respectively. The calibration curves in wide concentration ranges were linear with the coefficient of determination (r^2) greater than 0.99. Limits of detection (LOD) and quantification (LOQ) define the concentrations of analyte in those signal-to-noise ratios are equal to 3 and 10, respectively. The range of LOD values for PAAs was 0.50–0.82 μg L^{-1} and LOQ values also ranged from 1.6 to 2.5 μg L^{-1}. To evaluate precision of the proposed method, repeatability of the results of both intra- and inter-day experiments should be assessed. Relative standard deviation (RSD) was calculated at the concentrations of approximately 5, 25, and 125 times of LOQ. Intra-day precisions ($n = 6$) were less than or equal to 1.1, 1.4, and 2.7% at the concentrations of 200, 40, and 10 μg L^{-1}, respectively. Also, inter-day precisions (16 measurements in 4 successive days, 4 measurements in each day) in the concentrations mentioned above were less than or equal to 2.5, 3.7, and 5.1%, respectively.

Real samples analysis

This section aimed to examine the impact of eliminating the real sample matrix on relative recovery percent (RR%) values. In this context, following spiking 10, 50, and 250 μg L^{-1} of each amine to real samples and deionized water, clean up and the simultaneous extraction and derivatization processes were executed by the established method. For the second time, all the previously mentioned steps were followed, with the exception that both the real samples and deionized water were exposed to the adsorbent. The RR% values were computed based on Eq. (4) and presented in Table 2. The RR% values obtained from skin moisturizer samples (#1, #2, and #3), after matrix elimination or decrease, were 101–110, 95–112, and 100–105%, respectively. It should be noted that, without using clean up step, these figures were 100–128, 110–130, and 95–128%, respectively. Thus, it can be inferred that eliminating or decreasing the matrix effect of samples has successfully diminished the major impacts of the matrix on the extraction and derivatization processes, making this method as a reliable approach for analyzing the studied compounds. The chromatograms obtained from the GC-FID analysis of skin moisturizer samples exhibited no doubtful peaks in the retention times of the analytes. This finding indicated that none of the examined PAAs was detected in skin moisturizers at the concentrations equal to or exceeding the LODs established by the analytical method.

Comparison with other approaches

Based on the findings shown in Table 3, the proposed method exhibits high ERs (%) and EFs, and wider linear range values along with notable linearity compared to the other methods. Based on RSD (%) values, it can be asserted that this technique is highly consistent, repeatable, and fully competitive with alternative methods. Utilizing an external magnetic field to detach the MAA@Fe_3O_4 from the aqueous solution has significantly reduced the analysis time for PAAs. The LOQ and LOD values are less than or at least equal to the majority of the analytical methods. The application of BCF rendered this method less toxic, very effective, and exhibited good chromatographic characteristics, indicating that this method is better than or equal to similar methods.

Greenness of the method

The eco-friendliness of a method plays a key role in minimizing environmental harm, enhancing safety, lowering costs, and making chemical processes more sustainable. In this study, two approaches were employed to assess this aspect.

Complementary green analytical method index (ComplexGAPI) assessment

To gain a thorough understanding of how well the proposed method aligns with green chemistry principles, the ComplexGAPI tool was utilized. The resulting pictogram is color-coded with green, yellow, and red, representing high, moderate, and low levels of environmental, safety, and economic compatibility, respectively. Figure S8 provides a visual summary of this assessment for the developed method. Key advantages of this approach include

Analyte	LOD[a]	LOQ[b]	LR[c]	r^{2d}	RSD %[e] at the concentrations of						EF ± SD[f]	ER% ± SD[g]	UP% ± SD[h]
					10 μg L^{-1}		40 μg L^{-1}		μg L^{-1} 200				
					Intra-day	Inter-day	Intra-day	Inter-day	Intra-day	Inter-day			
PrA	0.50	1.6	1.6–10,000	0.9991	1.6	2.4	0.9	2.0	0.9	1.9	420 ± 5	84 ± 1	96 ± 2
sec-BuA	0.65	2.1	2.1–10,000	0.9989	1.9	3.0	1.0	2.1	1.0	2.0	495 ± 10	99 ± 2	96 ± 2
BuA	0.51	1.6	1.6–10,000	0.9993	1.4	2.9	0.9	1.8	0.8	1.8	485 ± 5	97 ± 1	92 ± 1
PeA	0.74	2.4	2.4–10,000	0.9995	2.0	3.8	1.1	2.3	1.0	2.1	510 ± 10	102 ± 2	92 ± 2
BeA	0.82	2.5	2.5–10,000	0.9995	2.7	5.1	1.4	3.7	1.1	2.5	525 ± 15	105 ± 3	97 ± 3

Table 1. Quantitative features of the developed DμSPE-VALLME-GC-FID method. [a]Limit of detection ($S/N = 3$) (μg L^{-1}). [b]Limit of quantification ($S/N = 10$) (μg L^{-1}). [c]Linear range (μg L^{-1}). [d]Coefficient of determination. [e]Relative standard deviation for intra- ($n = 6$) and inter-day ($n = 4$) precisions. [f]Enrichment factor ± standard deviation ($n = 3$). [g]Extraction recovery percentage ± standard deviation ($n = 3$). [h]Unadsorbed percentage ± standard deviation ($n = 3$).

Analyte	Mean relative recovery% ± standard deviation ($n=3$)					
	Before eliminating the matrix			After eliminating the matrix		
	Skin moisturizer #1	Skin moisturizer #2	Skin moisturizer #3	Skin moisturizer #1	Skin moisturizer #2	Skin moisturizer #3
The samples were spiked with each analyte at a concentration of 10 μg L^{-1}						
PrA	125 ± 2	130 ± 2	127 ± 2	102 ± 2	99 ± 2	101 ± 2
sec-BuA	128 ± 2	127 ± 2	128 ± 2	101 ± 2	95 ± 2	105 ± 2
BuA	128 ± 2	129 ± 2	123 ± 2	105 ± 1	104 ± 1	103 ± 1
PeA	123 ± 2	125 ± 2	128 ± 3	108 ± 2	110 ± 2	100 ± 2
BeA	126 ± 3	119 ± 3	128 ± 3	110 ± 3	110 ± 3	101 ± 3
The samples were spiked with each analyte at a concentration of 50 μg L^{-1}						
PrA	100 ± 2	110 ± 2	95 ± 2	106 ± 2	100 ± 2	100 ± 2
sec-BuA	119 ± 2	125 ± 2	124 ± 2	102 ± 2	98 ± 2	105 ± 2
BuA	125 ± 2	130 ± 2	126 ± 2	109 ± 2	110 ± 2	105 ± 1
PeA	125 ± 2	129 ± 3	128 ± 3	103 ± 2	112 ± 2	100 ± 2
BeA	128 ± 3	127 ± 3	128 ± 3	105 ± 3	112 ± 3	104 ± 3
The samples were spiked with each analyte at a concentration of 250 μg L^{-1}						
PrA	121 ± 2	125 ± 2	120 ± 2	107 ± 2	98 ± 2	105 ± 2
sec-BuA	128 ± 2	128 ± 2	126 ± 2	101 ± 2	100 ± 2	100 ± 2
BuA	122 ± 2	130 ± 2	123 ± 2	110 ± 2	106 ± 1	103 ± 1
PeA	126 ± 3	130 ± 3	128 ± 3	109 ± 2	112 ± 2	105 ± 2
BeA	125 ± 3	126 ± 3	128 ± 3	110 ± 3	110 ± 3	102 ± 3

Table 2. Study of matrix effect in the samples spiked at different concentrations (without dilution).

simple sample preparation, minimal solvent usage, absence of harmful vapor emissions, strong performance in quantitative and qualitative analyses, adherence to environmental sustainability principles, and lower safety and health risks.

Analytical eco-scale (AES) assessment

In this study, the AES (Green Analysis Evaluation Score) tool was used to assess the environmental impact and greenness of the proposed method. The tool works by assigning penalty points to different aspects of the analytical process that do not fully comply with the principles of ideal green methods. These penalty points are given for factors such as the amount of reagents used, hazards associated with the reagents and solvents, energy consumption, and the waste generated. In the AES system, a perfect green method scores 100 points. The final greenness score of a method is determined by subtracting the total penalty points from 100. The resulting score is categorized as follows: A score above 75 indicates excellent green analysis, a score above 50 indicates acceptable green analysis and a score below 50 indicates insufficient green analysis. As reported in Table 4, the AES score of the proposed method in this study is 82. This score suggests that the method is considered to have acceptable greenness, making it a suitable choice for environmentally conscious applications.

Conclusions

In this study, an innovative DμSPE-VALLME methodology was presented for the first time, aimed to eliminate or decrease matrix effect associated with skin moisturizing samples, thereby facilitating the derivatization and concurrent extraction of PAAs without interference from matrix effects. In this context, MAA@Fe_3O_4 adsorbent was employed for the first time in the clean up samples. BCF was utilized for the derivatization of PAAs in an alkaline medium. Application of the magnetic adsorbent enabled the facile collection of the adsorbent in the presence of an external magnetic field, obviating the necessity for centrifuge, which resulted in a reduction of the analysis duration. Throughout the analytical process, organic solvents were employed at μL-volumes, thereby characterizing this methodology as a green and environmentally sustainable approach. The analytical parameters associated with this technique, which included broad linear ranges (2.5–10,000 μg L^{-1}), low LODs (0.50–0.82 μg L^{-1}) and LOQs (1.6–2.5 μg L^{-1}), high EFs (420–525), significant r^2 values (0.9989–0.9995), and excellent ERs% (84–105%), contribute to the comprehensive or relative superiority of this method over existing methodologies. Moreover, the elimination or decreasing matrix effect of skin moisturizing samples has effectively mitigated both extraction and derivatization processes, rendering this methodology as a credible approach for the analysis of the selected compounds.

Method	Sample	Analyte	Derivatization reagent	LOD [a]	LOQ [b]	RSD [c]	LR [d]	r^2 [e]	EF[f]	ER% [g]	Ref.
HS-SDME-GC-MS [h]	Wastewater	PrA	Pentafluoro benzaldehyde	0.9	–	7.6	–	0.992	–	–	39
		BuA		0.7	–	5.3	–	0.995	–	–	
		PeA		0.8	–	9.8	–	0.997	–	–	
AALLME-GC-FID [i]	Well, river, tap waters, and wastewater	PrA	Butyl chloroformate	1.1	3.7	2.7	3.7–5000	0991	315	63	27
		sec-BuA		1.7	5.7	2.1	5.7–5000	0.992	266	53	
		BuA		0.4	1.4	3.6	1.4–5000	0.994	250	50	
		PeA		0.3	1.0	3.7	1.0–5000	0.996	360	72	
SPME-GC-FID [j]	Lake water	PrA	N-succinimidylbenzoate	0.17	–	2.4	1–1000	0.9920	–	–	40
		BuA		0.13	–	1.1	1–1000	0.9938	–	–	
		PeA		0.16	–	1.3	1–1000	0.9956	–	–	
HF-LPME-GC-MS [k]	River water	PrA	Pentafluoro benzaldehyde	0.29	–	6.7	–	0.995	172	–	41
		BuA		0.37	–	5.2	–	0.993	205	–	
		PeA		0.32	–	4.9	–	0.998	244	–	
DLLME-SFO-HPLC-DAD [l]	Well, river, and sea waters and wastewater	BuA	Phenyl isothiocyanate	0.01	–	< 12.5	0.1–500	0.994	210	–	30
		PeA		0.006	–		0.05–500	0.997	287	–	
SPME-GC-MS [m]	Fountain, tap, and surface waters	PrA	Pentafluoro benzaldehyde	1	5	5	5–500	0.9989	–	–	42
LLE-GC-MS [n]	Surface water and wastewater	PrA	Trichloroethylene	0.15	–	7.5	–	0.9967	–	–	43
		PeA	chloroformate	0.04	–	2.0	–	0.9998	–	–	
DμSPE-VALLME-GC-FID [o]	Skin moisturizer	PrA	Butyl chloroformate	0.50	1.6	1.6	$1.6–10^4$	0.9991	420	84 99	This work
		sec-BuA		0.65	2.1	1.9	$2.1–10^4$	0.9989	495		
		BuA		0.51	1.6	1.4	$1.6–10^4$	0.9993	485	97	
		PeA		0.74	2.4	2.0	$2.4–10^4$	0.9995	510	102	
		BeA		0.82	2.5	2.7	$2.5–10^4$	0.9995	525	105	

Table 3. Comparison of the development method with similar approaches for derivatization, extraction, and determination of PAAs. [a]Limit of detection (μg L^{-1}). [b]Limit of quantification (μg L^{-1}). [c]Relative standard deviation (%). [d]Linear Range (μg L^{-1}). [e]Coefficient of determination. [f]Enrichment factor. [g]Extraction recovery percentage. [h]Head space-single drop microextraction-gas chromatography-mass spectrometry. [i]Air-assisted liquid-liquid microextraction-gas chromatography-flame ionization detection. [j]Solid phase microextraction-gas chromatography-flame ionization detection. [k]Hollow fiber-liquid phase microextraction-gas chromatography-mass spectrometry. [l]Dispersive liquid-liquid microextraction based on solidification of floating organic droplet-high performance liquid chromatography-diode array detection. [m]Solid phase microextraction-gas chromatography-mass spectrometry. [n]Liquid-liquid extraction-gas chromatography-mass spectrometry. [o]Dispersive micro solid phase extraction - vortex-assisted liquid-liquid microextraction-gas chromatography-flame ionization detection.

Reagents	Penalty points (PPs)
DμSPE-VALLME-GC-FID	
1,1,2-TCE (15μL)	4
BCF (5μL)	4
EDTA (10 mg)	2
MAA@Fe_3O_4	1
NaCl	1
NaOH	1
Deionized water	0
MAA@Fe_3O_4 recycling	+ 1
	12Σ
Instruments	
GC-FID	2
Vortex	1
Centrifuge	1
pH-meter	1
Waste	1
	6Σ
Total PPs	18
AES Score	82

Table 4. Evaluation of the greenness of the proposed method using analytical Eco-Scale (AES) approach.

Data availability

All data generated or analyzed during this study are included in this published article. This data is provided within the manuscript or supplementary information files.

Received: 15 January 2025; Accepted: 3 March 2025
Published online: 17 March 2025

References

1. Fekete, A., Malik, A. K., Kumar, A. & Schmitt-Kopplin, P. Amines in the environment. *Crit. Rev. Anal. Chem.* **40**, 102–121 (2010).
2. Jang, J. K. Amines as occupational hazards for visual disturbance. *Ind. Health.* **54**, 101–115 (2016).
3. Cowell, A. *An Investigation into the Synthesis, Structural Characterisation, Thermal and Polymorphic Behaviour of Organic Crystalline Materials* (University of Birmingham, 2011).
4. Bhat, A. P. & Gogate, P. R. Degradation of nitrogen-containing hazardous compounds using advanced oxidation processes: A review on aliphatic and aromatic amines, dyes, and pesticides. *J. Hazard. Mater.* **403**, 123657 (2021).
5. Gong, W. L., Sears, K. J., Alleman, J. E. & Blatchley, E. R. III Toxicity of model aliphatic amines and their chlorinated forms. *Environ. Toxicol. Chemistry: Int. J.* **23**, 239–244 (2004).
6. Kaykhaii, M., Nazari, S. & Chamsaz, M. Determination of aliphatic amines in water by gas chromatography using headspace solvent Microextraction. *Talanta* **65**, 223–228 (2005).
7. Malinowski, S., Wróbel, M. & Woszuk, A. Quantum chemical analysis of the corrosion Inhibition potential by aliphatic amines. *Materials* **14**, 6197 (2021).
8. Marzo, A., Monti, N., Ripamonti, M., Muck, S. & Martelli, E. A. Determination of aliphatic amines by gas and high-performance liquid chromatography. *J. Chromatogr. A.* **507**, 241–245 (1990).
9. Gagnaire, F. et al. Nasal irritation and pulmonary toxicity of aliphatic amines in mice. *J. Appl. Toxicol.* **9**, 301–304 (1989).
10. Verdú-Andrés, J., Campins-Falco, P. & Herráez-Hernández, R. Determination of aliphatic amines in water by liquid chromatography using solid-phase extraction cartridges for preconcentration and derivatization. *Analyst* **126**, 1683–1688 (2001).
11. Moliner-Martínez, Y., Herráez-Hernández, R. & Campíns-Falcó, P. A microanalytical method for ammonium and short-chain primary aliphatic amines using precolumn derivatization and capillary liquid chromatography. *J. Chromatogr. A.* **1164**, 329–333 (2007).
12. Choi, N. R., Lee, J. Y., Ahn, Y. G. & Kim, Y. P. Determination of atmospheric amines at Seoul, South Korea via gas chromatography/tandem mass spectrometry. *Chemosphere* **258**, 127367 (2020).
13. Sha, Y., Meng, J., Lin, H., Deng, C. & Liu, B. Development of single-drop Microextraction and simultaneous derivatization followed by GC-MS for the determination of aliphatic amines in tobacco. *J. Sep. Sci.* **33**, 1283–1287 (2010).
14. Zhang, H., Ren, S., Yu, J. & Yang, M. Occurrence of selected aliphatic amines in source water of major cities in China. *J. Environ. Sci.* **24**, 1885–1890 (2012).
15. Cao, L. W., Wang, H., Li, J. S. & Zhang, H. S. 6-Oxy-(N-succinimidyl acetate)-9-(2′-methoxycarbonyl) fluorescein as a new fluorescent labeling reagent for aliphatic amines in environmental and food samples using high-performance liquid chromatography. *J. Chromatogr. A.* **1063**, 143–151 (2005).
16. Lamba, S. et al. Determination of aliphatic amines by high-performance liquid chromatography-amperometric detection after derivatization with naphthalene-2, 3-dicarboxaldehyde. *Anal. Chim. Acta*. **614**, 190–195 (2008).
17. Cao, L. W., Wang, H., Liu, X. & Zhang, H. S. Spectrofluorimetric determination of aliphatic amines using a new fluorigenic reagent: 2, 6-dimethylquinoline-4-(N-succinimidyl)-formate. *Talanta* **59**, 973–979 (2003).
18. Kambia, K. et al. High-performance liquid chromatographic method for the determination of Di (2-ethylhexyl) phthalate in total parenteral nutrition and in plasma. *J. Chromatogr. B Biomed. Sci. Appl.* **755**, 297–303 (2001).
19. Cai, Y. Q., Jiang, G. B., Liu, J. F. & Zhou, Q. X. Multi-walled carbon nanotubes packed cartridge for the solid-phase extraction of several phthalate esters from water samples and their determination by high-performance liquid chromatography. *Anal. Chim. Acta*. **494**, 149–156 (2003).

20. Batlle, R. & Nerín, C. Application of single-drop Microextraction to the determination of dialkyl phthalate esters in food simulants. *J. Chromatogr. A*. **1045**, 29–35 (2004).
21. González-Sálamo, J., González-Curbelo, M. Á., Socas-Rodríguez, B., Hernández-Borges, J. & Rodríguez-Delgado, M. Á. Determination of phthalic acid esters in water samples by Hollow fiber liquid-phase Microextraction prior to gas chromatography-tandem mass spectrometry. *Chemosphere* **201**, 254–261 (2018).
22. Holadová, K., Prokůpková, G., Hajšlová, J. & Poustka, J. Headspace solid-phase Microextraction of phthalic acid esters from vegetable oil employing solvent based matrix modification. *Anal. Chim. Acta*. **582**, 24–33 (2007).
23. Jagirani, M. S. & Soylak, M. A. Recent advances in solid-phase Microextraction of toxic pollutants using nanotechnology scenario. *Microchem. J.* **159**, 105436 (2020).
24. Penalver, A., Pocurull, E., Borrull, F. & Marce, R. Determination of phthalate esters in water samples by solid-phase Microextraction and gas chromatography with mass spectrometric detection. *J. Chromatogr. A*. **872**, 191–201 (2000).
25. Liang, P., Xu, J. & Li, Q. Application of dispersive liquid-liquid Microextraction and high-performance liquid chromatography for the determination of three phthalate esters in water samples. *Anal. Chim. Acta*. **609**, 53–58 (2008).
26. Quigley, A., Cummins, W. & Connolly, D. Dispersive liquid-liquid Microextraction in the analysis of milk and dairy products: A review. *J. Chem*. **4040165** (2016).
27. Farajzadeh, M. A. & Nouri, N. Simultaneous derivatization and air-assisted liquid-liquid Microextraction of some aliphatic amines in different aqueous samples followed by gas chromatography-flame ionization detection. *Anal. Chim. Acta*. **775**, 50–57 (2013).
28. Chang, W. Y., Wang, C. Y., Jan, J. L., Lo, Y. S. & Wu, C. H. Vortex-assisted liquid-liquid Microextraction coupled with derivatization for the fluorometric determination of aliphatic amines. *J. Chromatogr. A*. **1248**, 41–47 (2012).
29. Wang, C. Y. et al. Sensitivity enhancement in the fluorometric determination of aliphatic amines using naphthalene-2, 3-dicarboxaldehyde derivatization followed by vortex-assisted liquid–liquid Microextraction. *Talanta* **152**, 475–481 (2016).
30. Kamarei, F., Ebrahimzadeh, H. & Asgharinezhad, A. A. Optimization of simultaneous derivatization and extraction of aliphatic amines in water samples with dispersive liquid–liquid Microextraction followed by HPLC. *J. Sep. Sci.* **34**, 2719–2725 (2011).
31. Halket, J. M. & Zaikin, V. G. Derivatization in mass spectrometry—1. Silylation. *Eur. J. Mass Spectrom.* **9**, 1–21 (2003).
32. Baker, G. B., Coutts, R. T. & Holt, A. Derivatization with acetic anhydride: applications to the analysis of biogenic amines and psychiatric drugs by gas chromatography and mass spectrometry. *J. Pharmacol. Toxicol. Methods*. **31**, 141–148 (1994).
33. Tzanavaras, P. D. *Derivatization in Analytical Chemistry* (MDPI-Multidisciplinary Digital Publishing Institute, 2022).
34. Kataoka, H. Derivatization reactions for the determination of amines by gas chromatography and their applications in environmental analysis. *J. Chromatogr. A*. **733**, 19–34 (1996).
35. Hušek, P. Chloroformates in gas chromatography as general purpose derivatizing agents. *J. Chromatogr. B Biomed. Sci. Appl.* **717**, 57–91 (1998).
36. Qiao, J., Wang, M., Yan, H. & Yang, G. Dispersive solid-phase extraction based on magnetic dummy molecularly imprinted microspheres for selective screening of phthalates in plastic bottled beverages. *J. Agric. Food Chem.* **62**, 2782–2789 (2014).
37. Farajzadeh, M. A., Fazli, N., Pezhhanfar, S. & Mogaddam, M. R. A. Facile and rapid Preparation of magnetic Octadecylamine nanocomposite and its application as a capable adsorbent in magnetic dispersive solid phase extraction of some polycyclic aromatic hydrocarbons from wastewater samples. *Chem. Pap.* **77**, 781–794 (2023).
38. Farajzadeh, M. A., MohammadMehri, S. & Mogaddam, M. R. A. Application of core-shell magnetic metal-organic framework in developing dispersive micro solid phase extraction combined with dispersive liquid-liquid Microextraction for the extraction and enrichment of some pesticides in orange blossom, Aloysia Citrodora, and fennel herbal infusions. *J. Chromatogr. A* 465608 (2024).
39. Deng, C., Li, N., Wang, L. & Zhang, X. Development of gas chromatography–mass spectrometry following headspace single-drop Microextraction and simultaneous derivatization for fast determination of short-chain aliphatic amines in water samples. *J. Chromatogr. A*. **1131**, 45–50 (2006).
40. Zhao, Y. Y. et al. Determination of aliphatic amines using N-succinimidyl benzoate as a new derivatization reagent in gas chromatography combined with solid-phase Microextraction. *J. Chromatogr. A*. **1021**, 175–181 (2003).
41. Chia, K. J. & Huang, S. D. Simultaneous derivatization and extraction of primary amines in river water with dynamic Hollow fiber liquid-phase Microextraction followed by gas chromatography-mass spectrometric detection. *J. Chromatogr. A*. **1103**, 158–161 (2006).
42. Gionfriddo, E., Passarini, A. & Pawliszyn, J. A facile and fully automated on-fiber derivatization protocol for direct analysis of short-chain aliphatic amines using a matrix-compatible solid-phase Microextraction coating. *J. Chromatogr. A*. **1457**, 22–28 (2016).
43. Pietsch, J., Hampel, S., Schmidt, W., Brauch, H. J. & Worch, E. Determination of aliphatic and alicyclic amines in water by gas and liquid chromatography after derivatization by chloroformates. *Fresenius's J. Anal. Chem.* **355**, 164–173 (1996).

Acknowledgements

The authors are thankful to the University of Tabriz for financial support.

Author contributions

M.A.F. performed the analytical methodology and edited the manuscript.S.M.M. performed adsorbent synthesis, methodology and characterization, analytical analysis and methodology, data analysis, software applications, and manuscript writing.M.R.A.M. edited the manuscript.

Declarations

Competing interests

The authors declare no competing interests.

Additional information

Supplementary Information The online version contains supplementary material available at https://doi.org/10.1038/s41598-025-92919-4.

Correspondence and requests for materials should be addressed to M.A.F.